

A Severity-Aware Reliability Index for Risk-Informed Structural Design

MOUSSA LEBLOUBA^{*1}, SAMER BARAKAT², and RAGHAD AWAD¹

¹*Department of Civil & Environmental Engineering, College of Engineering, University of Sharjah,
P.O.Box 27272, University City, Sharjah, UAE*

²*Civil Engineering Department, Fahad Bin Sultan University, Tabuk, Saudi Arabia*

August 19, 2025

Abstract

Classical measures of structural reliability, such as the probability of failure and the related reliability index, are still widely applied in practice. However, these measures are frequency-based only, and they do not give information about the severity of failure once it happens. This missing aspect can cause underestimation of risks, in particular when rare events produce very undesirable consequences. In this paper, a new reliability framework is proposed to address this issue. The framework is based on a new concept, called the Expected Failure Deficit (EFD), which is defined as the average deficiency of the system response when failure occurs. From this quantity, a new reliability index is introduced, called the Severity-Aware Reliability Index, which evaluates the consequence of failure in comparison with the Gaussian benchmark. The mathematical formulation is derived and it is shown that the inverse mapping exists in a restricted domain, which can be interpreted as an indicator of excessive tail risks. A Severity Classification System with five levels is also proposed and calibrated from analytical expressions. Numerical examples, including Gaussian, mildly nonlinear, and heavy-tailed cases, demonstrate that the proposed framework agrees with classical measures in standard situations, while being able to detect hidden severity in more complex cases. The method can therefore be used not only to quantify severity of failure, but also to classify risks in support of engineering design.

Keywords: Structural reliability, Failure probability, Reliability index, Failure severity, Expected Failure Deficit, Risk-informed design, Tail behavior, Limit-state function, Engineering safety

1. Introduction

The assurance of structural safety and reliability continues to be among the fundamental goals in civil engineering applications. While structural failures remain statistically rare events, their associated consequences may be of significant magnitude. Past failures, such as the collapse of the I-35W Mississippi River Bridge in 2007 or the Sampoong Department Store in 1995, are strong reminders of the catastrophic impacts that a single failure may

*Corresponding author: mleblouba@sharjah.ac.ae

produce in terms of human casualties, disruption of economic activity, and erosion of public trust.

These tragic events are not remembered due to their occurrence frequency, but rather due to the severity of their outcomes. Such events emphasize a crucial aspect in structural risk evaluations: the acceptability of a system depends not only on how likely the failure is, but also on what kind of failure happens when it occurs. A system that fails frequently but with minor consequences may still be tolerated. In contrast, a system that fails rarely but in a catastrophic manner is typically unacceptable. Therefore, any framework intended for reliability assessment that neglects the consequence aspect of failure may lead to incomplete or even misleading representation of risk.

As a response to these concerns, current structural design practices have adopted reliability-based approaches. In particular, the Load and Resistance Factor Design (LRFD) [1, 2] methodology has become the most widely implemented framework. In this context, partial safety factors are calibrated in such a way that specific target reliability levels are achieved. These targets are usually expressed in terms of a prescribed probability of failure, p_f , or its equivalent reliability index β [1, 3, 4]. For instance, for ordinary structural components, the reliability index is commonly set around $\beta = 3.5$, which corresponds approximately to a failure probability on the order of 10^{-4} per year [3, 5–9].

Traditional reliability measures, such as the failure probability p_f and the associated index β , remain central tools in both code calibration and design validation procedures. The index β is defined using the standard normal cumulative distribution function as $\beta = -\Phi^{-1}(p_f)$, and serves as a convenient way to translate probability information into a normalized reliability scale [10–14]. More advanced reliability indices, such as the Hasofer–Lind index, were also developed to achieve geometric invariance in reliability problems [15], yet they still rely on interpreting failure as a binary condition in which a limit-state threshold is crossed.

This binary-type interpretation presents one of the main limitations of classical reliability indices. Whether the structural limit is slightly exceeded or largely violated, both scenarios are assigned the same outcome: a failure has occurred. This means that the classical reliability metrics do not reflect how severe the failure was. For instance, a structure that experiences limited local yielding is treated the same as a complete structural collapse, as long as the same limit-state function is exceeded. This insensitivity to consequence has become a matter of increasing concern, especially in modern infrastructure systems that are subject to rare but extreme events, such as floods, impact loads, or accidental overloads [16].

In other disciplines, the importance of integrating the severity of outcomes into risk assessments has been acknowledged for several decades. In general risk theory, risk is often expressed as a combination of both the likelihood and the consequence of an undesirable event [17, 18]. In structural and insurance applications, expected loss models incorporate both the probability of occurrence and the associated severity [19, 20]. In mechanical systems, Failure Mode and Effects Analysis (FMEA) uses a risk metric that depends on the product of severity, occurrence, and detection likelihood [21].

The field of financial risk management has undergone a similar evolution. The classical Value-at-Risk (VaR) measure estimates the probability that a certain threshold is exceeded,

without accounting for the magnitude of excess loss [22]. On the other hand, Conditional Value-at-Risk (CVaR), also referred to as Expected Shortfall, addresses this limitation by considering the expected loss given that the threshold has been exceeded [23]. CVaR is now widely used because of its desirable mathematical properties and its capacity to account for tail risk in a more appropriate manner [24–26].

A common feature among all these examples is that systems or portfolios having equal failure probabilities may exhibit significantly different outcomes. When the analysis is purely based on frequency, both scenarios are considered similar from a reliability point of view. This limitation still remains unresolved in the majority of structural reliability formulations.

In this study, a new reliability index is proposed which explicitly considers the severity aspect of failure. The goal is not to change the classical reliability concept, but to extend it through the introduction of an additional index that accounts for how bad the failure is when it occurs. The idea originates from a natural question: *“If the system under investigation is replaced with an equivalent Gaussian system, then what level of reliability would result in the same average consequence under failure?”*

Answering this question leads to a new severity-aware reliability index, which may be interpreted as a complement to the classical β index. The new index is derived through a probabilistic formulation that incorporates the severity of failure events in a systematic manner. The construction starts from a new quantity, introduced in this paper and referred to as the Expected Failure Deficit (EFD). Once normalized and mapped to the Gaussian domain, this quantity provides a meaningful basis for defining severity-aware reliability classes.

This study includes four main contributions:

1. It introduces the Expected Failure Deficit and the associated severity-aware reliability index, which is benchmarked against an equivalent Gaussian behavior. This formulation extends the classical reliability concept by reflecting not only the frequency of failure but also the level of severity once failure occurs.
2. It derives and validates the mathematical properties of the proposed index, including its monotonicity, continuity, and bounded domain, and includes asymptotic derivations that support its theoretical consistency.
3. It shows that the domain restriction of the proposed index does not represent a drawback but rather acts as a diagnostic feature capable of detecting severe tail behavior, for which equivalent Gaussian interpretation is no longer meaningful.
4. It proposes a new Severity Classification System based on the normalized failure deficit, which defines five severity levels ranging from mild to extreme. The classification thresholds are derived analytically and are linked to classical β -based benchmarks. This system allows engineers to interpret severity more clearly and supports informed decision-making in structural design.

The remainder of the paper is structured as follows: [Sec. 2](#) presents the mathematical formulation of the Expected Failure Deficit and the corresponding severity-aware index. [Sec. 3](#) analyzes the properties of the transformation and discusses how tail effects are handled. [Sec. 4](#) contains numerical applications that demonstrate the behavior of the

new index using synthetic and realistic examples. [Sec. 5](#) develops the proposed severity classification and integrates it into a practical workflow. [Sec. 6](#) provides a thorough discussion, implications in engineering design, and directions for future extensions of our work.

2. Conceptual Basis for the Severity-Aware Index

In this, we introduce the mathematical formulation that motivates the proposed severity-aware reliability index. First, the classical definitions used in structural reliability are briefly recalled to establish the foundational context. Then, a new quantity, the expected failure deficit, E_f , is introduced and normalized to obtain a dimensionless, transferable measure of severity, E_f^* . This leads to the formulation of a new reliability index, denoted β_S , which encapsulates both the frequency and severity of structural failures.

2.1. Classical Framework and Notation

Let $\mathbf{X} = (X_1, X_2, \dots, X_n)$ represent a vector of basic random variables describing uncertainties in the structural system, such as loads, material properties, and geometric dimensions. The performance of the structure is modeled through a limit-state function $g(\mathbf{X})$, with $g(\mathbf{X}) \geq 0$ indicates a safe state and $g(\mathbf{X}) < 0$ denotes failure. The failure domain is thus defined as:

$$\mathcal{F} = \mathbf{X} \in \mathbb{R}^n \mid g(\mathbf{X}) < 0.$$

The probability of failure, p_f , is given by:

$$p_f = \mathbb{P}(g(\mathbf{X}) < 0) = \int_{\{x \mid g(x) < 0\}} f_{\mathbf{X}}(x) dx,$$

where $f_{\mathbf{X}}(x)$ is the joint density function of \mathbf{X} . In many practical problems, the First-Order Reliability Method (FORM) is used to approximate this probability efficiently.

The reliability index β is traditionally defined by the inverse of the standard normal cumulative distribution:

$$\beta = -\Phi^{-1}(p_f),$$

and, in the special case where $g(\mathbf{X}) \sim \mathcal{N}(\mu_g, \sigma_g^2)$, the reliability index becomes:

$$\beta = \frac{\mu_g}{\sigma_g}.$$

2.2. Expected Failure Deficit and Normalization

Conventional measures such as p_f and β only characterize the frequency of failure, not its magnitude. However, in practice, the depth of failure (i.e., how far into the unsafe region the structure enters) is also critical. To incorporate this, we define the Expected Failure Deficit as:

$$E_f = \mathbb{E}[-g(\mathbf{X}) \mid g(\mathbf{X}) < 0], \quad (1)$$

which expresses the average shortfall conditional on failure.

To make this measure scale-invariant and comparable across different systems, it is normalized by the standard deviation of the limit-state function:

$$E_f^* = \frac{E_f}{\sigma_g}. \quad (2)$$

This normalization parallels the classical reliability index $\beta = \mu_g/\sigma_g$: both scale a mean effect by the global dispersion of g . In Gaussian settings, the normalized deficit has a closed form,

$$E_f^* = \frac{\varphi(\beta)}{\Phi(-\beta)} - \beta, \quad (3)$$

with φ and Φ the standard normal density and distribution. The mapping

$$F(b) := \frac{\varphi(b)}{\Phi(-b)} - b$$

is strictly decreasing for $b > 0$ with

$$\lim_{b \downarrow 0} F(b) = \frac{2}{\sqrt{2\pi}} \approx 0.7979, \quad \lim_{b \uparrow \infty} F(b) = 0,$$

so $F : (0, \infty) \rightarrow (0, 2/\sqrt{2\pi})$.

Interpretation. [Fig. 1](#) separates *how often* failure occurs (the area $\mathbb{P}\{g < 0\} = p_f$, which sets β via $p_f = \Phi(-\beta)$) from *how far* failures penetrate on average (EFD). The normalized deficit E_f^* places E_f on the same scale as the dispersion of g ; in Gaussian settings it is linked to $b = \mu_g/\sigma_g$ through [Eq. \(3\)](#). Because the Gaussian mapping $F(b) = \varphi(b)/\Phi(-b) - b$ is strictly decreasing with image $(0, 2/\sqrt{2\pi})$, larger tail severity corresponds to larger E_f^* , approaching the endpoint $2/\sqrt{2\pi}$.

Remark 2.1 (Standing assumption). We assume $g(\mathbf{X}) \in L^2$, i.e., $\sigma_g^2 = \text{Var}[g(\mathbf{X})] < \infty$, so that $E_f^* := \mathbb{E}[-g \mid g < 0]/\sigma_g$ is well-defined. We also tacitly assume $p_f = \mathbb{P}(g(\mathbf{X}) < 0) > 0$.

Remark 2.2 (Robust screening for taily systems). Because E_f^* divides by σ_g , the index requires $\sigma_g < \infty$. When tail behavior is uncertain, one may first screen with a robust scale (e.g., MAD or IQR) or with the conditional scale $\sigma_{g|g<0}$. This does not alter the main theory; it simply avoids undefined normalizations in infinite-variance regimes.

2.3. Monte Carlo illustration: same reliability, different expected failure deficit

To complement [Fig. 1](#), we consider two non-Gaussian scenarios with *matched* $p_f \approx 10^{-2}$ (thus nearly equal β) but different tail severities. In both cases $g = R - S + c$, where the constant shift c is calibrated so that $\mathbb{P}(g < 0) = p_f$. The set-up is:

- Scenario A (lighter failure tail): $R \sim \text{lognormal}$; $S \sim \text{Gumbel}$.
- Scenario B (heavier failure tail): same R ; $S \sim$ a mixture of Gumbels with a rare extreme component.

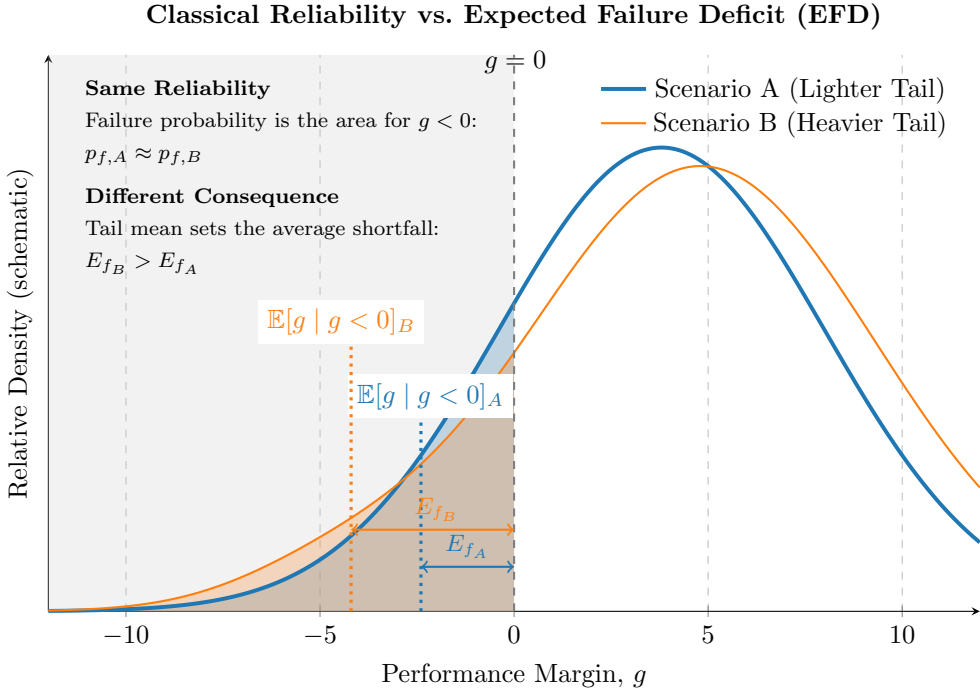


Figure 1. Schematic of the classical failure event and the expected failure deficit (EFD). The shaded half-plane is $g < 0$ (i.e., $S > R$). The dashed gray line marks $g = 0$. The tail conditional mean $\mathbb{E}[g | g < 0]$ locates the center of mass of the failure side, and the horizontal bracket shows $\text{EFD} = \mathbb{E}[-g | g < 0]$. Two systems can share the same p_f (thus the same β) yet have different EFD.

The results are shown in Figs. 2 and 3, and the overlays in Figs. 4 and 5. In each panel, the shaded half-plane is $g < 0$; the gray dashed line is $g = 0$; the colored dashed line marks the tail conditional mean $\mathbb{E}[g | g < 0]$; and the horizontal double-arrow from that line back to $g = 0$ visualizes the expected failure deficit $E_f = \mathbb{E}[-g | g < 0]$ (cf. Eq. (2)).

Numerical results. From MC runs with 10^6 samples per scenario:

$$\begin{aligned}
 \text{Scenario A: } & \mu_g = 4.148, \sigma_g = 1.390, p_f = 9.971 \times 10^{-3}, \beta = 2.327, \\
 & \mathbb{E}[g | g < 0] = -1.011, \quad E_f = 1.011, \quad E_f^* = E_f / \sigma_g = 0.727; \\
 \text{Scenario B: } & \mu_g = 4.352, \sigma_g = 1.468, p_f = 9.775 \times 10^{-3}, \beta = 2.335, \\
 & \mathbb{E}[g | g < 0] = -2.081, \quad E_f = 2.081, \quad E_f^* = 1.418.
 \end{aligned}$$

By construction $\mathbb{P}(g < 0)$ is (nearly) the same in A and B, hence β is (nearly) identical. What differs is the *average depth* into the failure region: Scenario B's EFD is about twice Scenario A's, visible as the longer orange bracket in the overlay (Fig. 5).

Relation to the Gaussian benchmark (diagnostic only). For Gaussian $g \sim \mathcal{N}(\mu_g, \sigma_g^2)$,

$$E_f^* = \frac{\varphi(\beta)}{\Phi(-\beta)} - \beta,$$

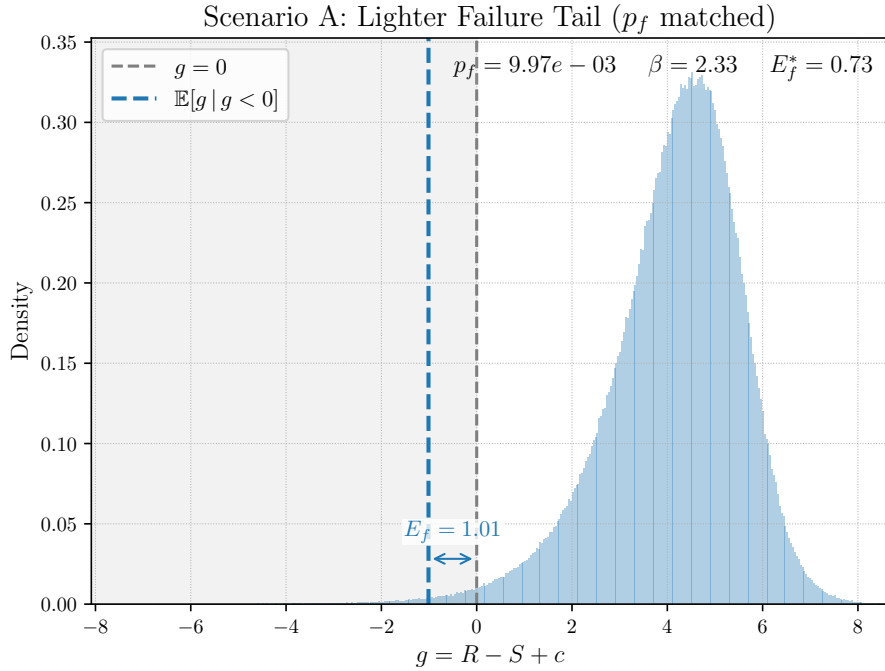


Figure 2. Scenario A (lognormal R ; Gumbel S), calibrated to $p_f \approx 9.97 \times 10^{-3}$ ($\beta \approx 2.33$). The curve shows the empirical density of $g = R - S + c$; the shaded half-plane marks the failure region $g < 0$; the dashed gray line is the boundary $g = 0$; the blue dashed line marks the tail conditional mean $\mathbb{E}[g | g < 0]$; and the blue double-arrow is the expected failure deficit $E_f = \mathbb{E}[-g | g < 0]$. Here $E_f \approx 1.01$ and $E_f^* = E_f / \sigma_g \approx 0.727$.

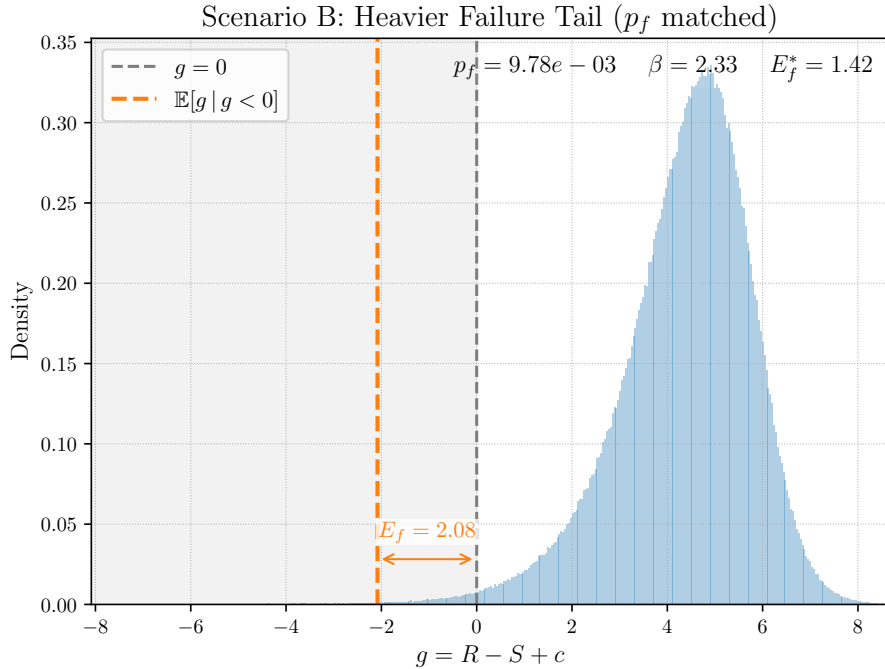


Figure 3. Scenario B (lognormal R ; mixture-Gumbel S with rare extremes), calibrated to $p_f \approx 9.78 \times 10^{-3}$ ($\beta \approx 2.33$). Visual elements as in [Fig. 2](#). The heavier failure tail shifts the tail mean further left, yielding a larger expected failure deficit: $E_f \approx 2.08$ and $E_f^* \approx 1.42$.

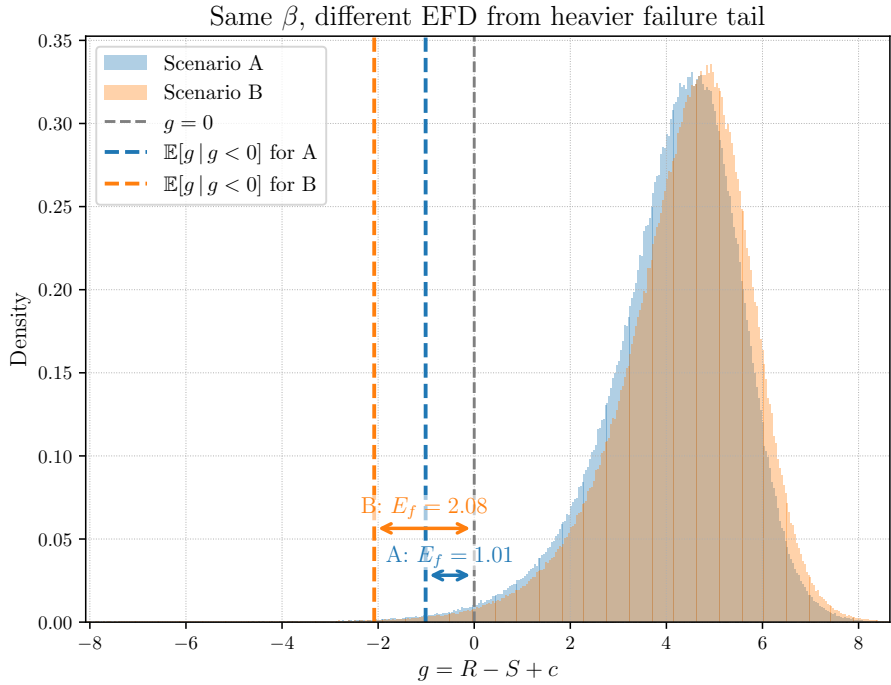


Figure 4. Overlay of Scenarios A (blue) and B (orange) with unified axes and shared binning. Both cases have the same failure probability (hence similar β), but the heavier tail in Scenario B pulls $\mathbb{E}[g | g < 0]$ farther left, producing a larger E_f (longer orange bracket). The dashed gray line is $g = 0$.

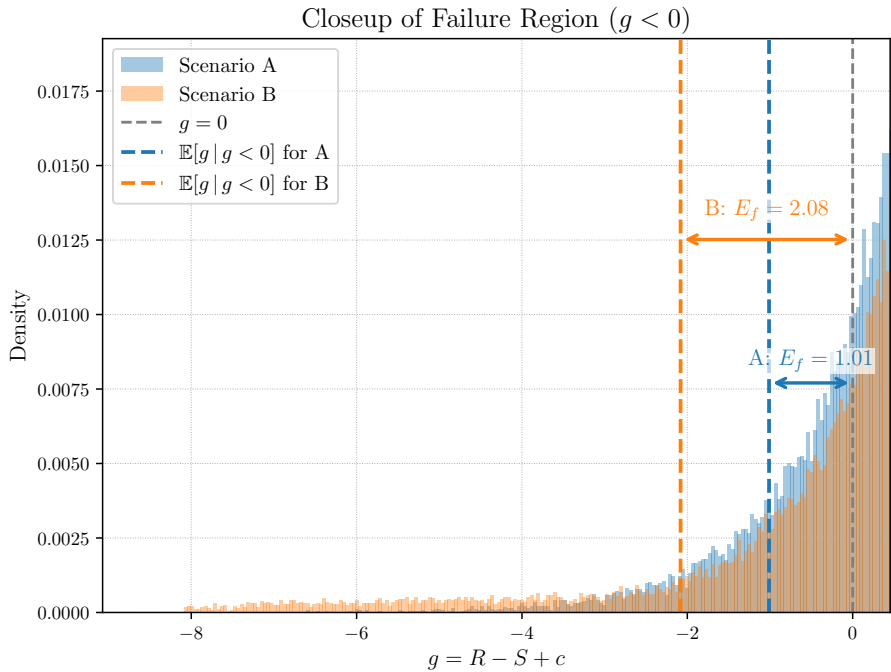


Figure 5. Close-up of the failure region $g < 0$ from the overlay: at matched p_f the tail conditional mean lies further into the unsafe side for Scenario B, so E_f is markedly larger than in Scenario A. This isolates the “how far” (E_f) distinction while holding the “how often” (p_f) essentially fixed.

so at $\beta \approx 2.33$ the Gaussian benchmark yields $E_f^* \approx 0.35$. Scenario A's $E_f^* = 0.727$ already exceeds this benchmark value (heavier failure tail than Gaussian at the same β), while Scenario B's $E_f^* = 1.418$ even exceeds the Gaussian *endpoint* $2/\sqrt{2\pi} \approx 0.798$, indicating behavior beyond what the Gaussian mapping can represent.

Design interpretation. The stress–strength probability $p_f = \mathbb{P}\{S > R\} = \mathbb{P}\{g < 0\}$ (and β) quantifies *how often* the boundary is crossed; EFD quantifies *how far* failures penetrate once they occur. For action effects with extreme-value/mixed behavior, two systems with the same p_f can have very different E_f (and E_f^*), as the A–B comparison shows. Reporting E_f^* alongside β therefore distinguishes designs with identical reliability but very different expected consequences in failure.

2.4. Severity-Aware Reliability Index

To incorporate both failure frequency and failure depth into a unified reliability metric, we introduce the Severity-Aware Reliability Index, β_S . This new index quantifies the equivalent Gaussian reliability level that would produce the same expected failure deficit as observed in the actual system.

Formally, we define β_S as the unique positive solution to the following nonlinear equation:

$$\frac{\varphi(\beta_S)}{\Phi(-\beta_S)} - \beta_S = E_f^* \quad (4)$$

This relationship inverts the analytical expression for E_f^* derived under the Gaussian assumption, and it ensures consistency: for systems whose limit-state function is Gaussian, we recover $\beta_S = \beta$. For other systems, β_S reflects the severity-equivalent reliability index that a Gaussian benchmark would require to yield the same average failure depth.

The defining function:

$$F(b) = \frac{\varphi(b)}{\Phi(-b)} - b \quad (5)$$

is strictly decreasing for $b > 0$, guaranteeing that the solution exists and is unique for any admissible value of E_f^* . This guarantees the well-posedness of the index and enables efficient computation using numerical solvers such as Newton–Raphson or bisection methods.

As a result, β_S serves not only as a severity-aware generalization of the classical reliability index β , but also as a diagnostic indicator of heavy-tailed or disproportionate failure behavior.

A summary of the core relationships presented in the section is provided in [Table 1](#).

2.5. Interpretation and Limiting Cases

The severity-aware index β_S should be interpreted as a back-calibrated reliability index that reflects not just how often failure occurs, but also how serious that failure is on average. A high β_S implies mild or shallow failure behavior, even if p_f is relatively large. Conversely, a low or undefined β_S indicates severe, heavy-tailed risk that classical measures cannot detect.

Table 1. Summary of core relationships

Expression	Description
$p_f = \Phi(-\beta)$	Failure probability
$\beta = \frac{\mu_g}{\sigma_g}$	Reliability index (Gaussian g)
$E_f = \mathbb{E}[-g(\mathbf{X}) \mid g(\mathbf{X}) < 0]$	Expected failure deficit
$E_f^* = \frac{E_f}{\sigma_g}$	Normalized deficit
$E_f^* = \frac{\varphi(\beta)}{\Phi(-\beta)} - \beta$	Closed-form for Gaussian system
$\beta_S : \frac{\varphi(b)}{\Phi(-b)} - b = E_f^*$	Severity-aware reliability index

This distinction gives rise to three conceptual cases:

Case I (Mild Failure): The system fails often, but the failure is shallow. In this case, $\beta_S > \beta$.

Case II (Gaussian-like Failure): The system exhibits failures with frequency and severity aligned. Here, $\beta_S \approx \beta$.

Case III (Catastrophic Tail Behavior): The system rarely fails, but when it does, the consequences are extreme. In this situation, $\beta_S < \beta$, or may be undefined.

These distinctions will be visualized in [Sec. 4](#).

3. Theoretical Analysis of the Proposed Reliability Measure

In this section we present the mathematical foundation and interpretive analysis of the proposed severity-aware reliability index β_S , introduced as a natural extension of the classical reliability index β . While β is uniquely determined by the probability of failure, β_S is defined through the normalized Expected Failure Deficit, E_f^* , and incorporates information about the conditional magnitude of failure. We aim here to (i) establish the conditions under which β_S is well-defined and unique, (ii) analyze its asymptotic properties and sensitivity, and (iii) recover the classical β in the Gaussian limit-state case. The analysis reveals not only the mathematical rigor of the formulation, but also its diagnostic power and interpretability in safety-critical applications.

3.1. Existence and Uniqueness of β_S

Recall that the new reliability measure β_S is defined as the unique positive solution to [Eq. \(4\)](#).

We now formally establish that such a solution always exists and is unique for any normalized expected deficit value $E_f^* \in (0, 2/\sqrt{2\pi})$.

Theorem 1 (Existence and Uniqueness). *Let*

$$F(b) = \frac{\varphi(b)}{\Phi(-b)} - b,$$

Then the following properties hold:

1. $F(b)$ is strictly decreasing on $(0, +\infty)$.
2. $\lim_{b \rightarrow 0^+} F(b) = \frac{2}{\sqrt{2\pi}} \approx 0.7979$.
3. $\lim_{b \rightarrow +\infty} F(b) = 0$.
4. The function $F : (0, \infty) \rightarrow (0, \frac{2}{\sqrt{2\pi}})$ is continuous and bijective.
5. For any normalized expected failure deficit $E_f^* \in (0, \frac{2}{\sqrt{2\pi}})$, there exists a unique value of $\beta_S > 0$ such that

$$F(\beta_S) = E_f^*.$$

Proof. We prove each part as follows:

Strict Monotonicity. Let $Z \sim \mathcal{N}(0, 1)$ and $r(b) := \mathbb{E}[Z \mid Z > b] = \varphi(b)/\Phi(-b)$. Then $F(b) = r(b) - b$ and $r'(b) = r(b) [r(b) - b]$ (quotient rule). Hence

$$F'(b) = r'(b) - 1 = r(b)F(b) - 1.$$

For the truncated normal,

$$\text{Var}(Z \mid Z > b) = 1 + b r(b) - r(b)^2 = 1 - r(b)F(b) > 0,$$

so $r(b)F(b) < 1$ and therefore $F'(b) < 0$ for all $b > 0$.

Asymptotic Behavior. As $b \rightarrow 0^+$,

$$F(b) \rightarrow \frac{\varphi(0)}{\Phi(0)} = \frac{1/\sqrt{2\pi}}{0.5} = \frac{2}{\sqrt{2\pi}} \approx 0.7979.$$

As $b \rightarrow \infty$, by the asymptotic expansion of Mills' ratio [27]:

$$F(b) = \frac{\varphi(b)}{\Phi(-b)} - b \sim \frac{1}{b} + \frac{1}{b^3} + O\left(\frac{1}{b^5}\right) \quad (b \rightarrow \infty) \Rightarrow F(b) \sim 0.$$

Continuity and Invertibility. Because $F(b)$ is continuous and strictly decreasing on $(0, \infty)$, and its image is $\left(0, \frac{2}{\sqrt{2\pi}}\right)$, it admits a unique inverse function

$$F^{-1} : \left(0, \frac{2}{\sqrt{2\pi}}\right) \rightarrow (0, \infty).$$

Therefore, for each $E_f^* \in (0, 0.7979)$, a unique β_S exists satisfying $F(\beta_S) = E_f^*$. \square

This result ensures that for any physically meaningful normalized deficit (i.e., $E_f^* < 0.7979$), a well-defined severity-aware index β_S exists and is unique. Notably, the upper limit of this domain is not merely a mathematical artifact but a fundamental diagnostic bound. If E_f^* exceeds this threshold, it signals that the observed severity lies beyond what any Gaussian failure model could explain. Such cases may indicate extreme-tailed behavior, structural brittleness, or regime shifts, each of which may warrant re-evaluation of the model or system design.

3.2. Asymptotic Behavior of $F(b)$

Understanding the behavior of $F(b)$ in limiting regimes enhances our interpretation of β_S in extreme cases.

Lemma 3.1 (Large b behavior). *As $b \rightarrow \infty$, we have [27]:*

$$F(b) = \frac{\varphi(b)}{\Phi(-b)} - b \sim \frac{1}{b} + \frac{1}{b^3} + O\left(\frac{1}{b^5}\right) \quad \text{as } b \rightarrow \infty$$

Thus:

$$\lim_{b \rightarrow \infty} F(b) = 0^+$$

This implies that systems with very high reliability (large β) are associated with extremely small normalized deficits, approaching zero. As expected, very safe systems also fail mildly, if at all.

Lemma 3.2 (Small b behavior). *As $b \rightarrow 0^+$:*

$$\varphi(-b) \rightarrow 0.5, \quad \Phi(b) \rightarrow \frac{1}{\sqrt{2\pi}}, \quad \Rightarrow \quad F(b) \rightarrow \frac{1}{0.5\sqrt{2\pi}} = \frac{2}{\sqrt{2\pi}}.$$

Hence, this maximum bound on E_f^* corresponds to a degenerate system where the performance margin is near zero and violations are large in magnitude on average.

These asymptotics not only validate the domain characterization but also assist in designing robust numerical solvers and preconditioners for computing β_S from given E_f^* values.

3.3. Sensitivity of β_S to Changes in Severity

From an engineering standpoint, it is essential to understand how sensitive the severity-aware index is to changes in the normalized failure deficit. This allows for interpreting β_S as a responsive diagnostic quantity.

Theorem 2 (Sensitivity of β_S). *Let β_S satisfy:*

$$F(\beta_S) = E_f^*.$$

Then:

$$\frac{d\beta_S}{dE_f^*} = \frac{1}{F'(\beta_S)} < 0.$$

Proof. By the Implicit Function Theorem, since F is continuously differentiable and $F'(\beta_S) < 0$ on $(0, \infty)$, we obtain:

$$\frac{d\beta_S}{dE_f^*} = \frac{1}{F'(\beta_S)} < 0.$$

□

The interpretation is immediate and important: as the average severity of failure increases, the corresponding severity-aware reliability index decreases. This behavior is consistent with the desired properties of a risk indicator. Moreover, the magnitude of this derivative may serve as an indicator of local sensitivity: flatter slopes imply that small changes in deficit produce large shifts in perceived reliability, a sign of structural fragility.

3.4. Consistency with the Gaussian Benchmark

We now revisit the canonical case where the limit-state function is Gaussian:

$$g(\mathbf{X}) \sim \mathcal{N}(\mu_g, \sigma_g^2).$$

In this setting:

- The classical reliability index is given by $\beta = \frac{\mu_g}{\sigma_g}$.
- The normalized failure deficit is:

$$E_f^* = \frac{\varphi(\beta)}{\Phi(-\beta)} - \beta.$$

But this is precisely the defining equation of β_S :

$$F(\beta_S) = E_f^* = F(\beta) \Rightarrow \beta_S = \beta.$$

This equivalence shows that β_S recovers the classical index exactly when Gaussianity holds. Consequently, β_S can be seen as a strict generalization of β : consistent under the ideal case and diagnostic under deviations.

3.5. Summary and Implications

The results established in this section demonstrate the mathematical integrity and operational clarity of the new reliability index:

- The function $F(b) = \frac{\varphi(b)}{\Phi(-b)} - b$ is continuous, strictly decreasing, and maps $(0, \infty)$ to $(0, \frac{2}{\sqrt{2\pi}})$.
- This mapping ensures that the inverse function defining β_S is unique and well-posed for any normalized failure deficit $E_f^* < 0.7979$.
- Asymptotic analysis reveals how β_S behaves in extreme regimes of reliability and severity.
- Sensitivity analysis confirms that β_S decreases monotonically with increasing severity, thereby making it suitable for practical diagnostics.
- In the Gaussian case, β_S reduces exactly to β , confirming backward compatibility and interpretability.

Engineering Implication The bounded domain of $F(b)$ is not a limitation, but a diagnostic asset. It signals when systems depart so far from Gaussian behavior (typically via heavy tails or extreme fragility) that even the proposed severity-aware metric reaches its expressive boundary. In such cases, β_S does not fail; it declares the model unfit for conventional calibration, prompting a deeper probabilistic reassessment or new modeling paradigms.

This theoretical foundation justifies the deployment of β_S in practical reliability studies and sets the stage for its application and validation through numerical experiments in the next section.

4. Numerical Investigation

This section is devoted to a series of numerical case studies developed to examine the interpretive capability and diagnostic strength of the proposed Severity-Aware Reliability Index, denoted as β_S . Each example has been carefully selected to illustrate a distinct aspect of the framework, starting from baseline theoretical consistency, moving to failure profiles characterized by non-critical consequences, and concluding with a configuration that contains rare but extremely severe failure events. The simulations are performed using Monte Carlo sampling, with a total of $N = 5,000,000$ realizations per case, thus, ensuring statistically stable estimates for all reliability metrics.

4.1. Example 1: Gaussian Benchmark – Validation Under Classical Assumptions

The first example serves to validate the proposed framework against classical reliability theory under ideal Gaussian conditions. The objective is to demonstrate that the severity-aware index β_S coincides with the traditional reliability index β when the underlying assumptions of normality are satisfied.

Problem Formulation

Consider a structural system governed by a linear limit-state function:

$$g(R, S) = R - S,$$

where the resistance R and the load S are independently distributed as follows:

$$R \sim \mathcal{N}(10, 1^2), \quad S \sim (5, 1.5^2).$$

Given that the sum of independent Gaussian variables is also Gaussian, the performance function $g(R, S)$ is itself normally distributed.

Results

$$\begin{aligned} \beta &= \frac{\mu_g}{\sigma_g} = \frac{\mu_R - \mu_S}{\sqrt{\sigma_R^2 + \sigma_S^2}} = \frac{10 - 5}{\sqrt{1^2 + (1.5)^2}} \approx 2.7735, \\ E_f^* &= \frac{\varphi(\beta)}{\Phi(-\beta)} - \beta \approx 0.3, \quad \beta_S = \beta. \end{aligned}$$

Or using Monte Carlo simulation, which yields almost the same reliability metrics:

$$\text{Classical Reliability Index: } \beta = 2.7748$$

$$\text{Normalized Expected Failure Deficit: } E_f^* = 0.3085$$

$$\text{Severity-Aware Index: } \beta_S = 2.6671$$

Interpretation

As expected, the two indices are in close numerical agreement, with a small discrepancy of approximately 3.9%. This deviation arises from inherent sampling noise and numerical approximation during root-finding. Importantly, both β and β_S indicate a low failure probability and moderate severity. This example confirms the internal consistency of the proposed metric under canonical assumptions and serves as a theoretical validation of the formulation.

4.2. Example 2: Mild Failure Case – Distinguishing Favorable Deficit Profiles

In this example, the performance function remains the same as in the previous case; however, the input distributions are altered to induce non-Gaussian behavior, particularly in the tails. This setup is intended to show how the proposed framework differentiates between systems with frequent but non-catastrophic failures and those with more hazardous profiles.

Problem Formulation

Assuming similar limit-state function $g(R, S) = R - S$, but the random variables are now specified as follows:

$$R \sim \text{Lognormal}(\mu_{\ln} = 2.3, \sigma_{\ln} = 0.2), \quad S \sim \text{Gumbel}(\mu = 8, \text{scale} = 1.2).$$

This configuration results in a higher probability of failure due to more dispersed loading, but with a resistance distribution skewed towards higher values, which moderates the severity of the failure events.

Results

Simulation yields:

$$\text{Classical Reliability Index:} \quad \beta = 1.5236$$

$$\text{Normalized Expected Failure Deficit:} \quad E_f^* = 0.3040$$

$$\text{Severity-Aware Index:} \quad \beta_S = 2.7219$$

Interpretation

The classical reliability index β indicates a relatively poor performance, corresponding to a failure probability of approximately 6.38%. However, the severity-aware index β_S is significantly higher, and in fact, closely matches the benchmark value from the Gaussian case in Example 1. This divergence signifies that, although failures occur frequently, they are of considerably less magnitude than would be expected under a Gaussian benchmark. Thus, the β_S index correctly identifies the favorable failure profile and avoids unduly penalizing systems that exhibit moderate deficits. This capability is of practical significance in systems where slight performance exceedances are tolerable or non-critical.

4.3. Example 3: Extreme Severity Case – Revealing Hidden Tail Risks

The third example explores the framework's diagnostic power in scenarios where rare but extremely severe failure events are embedded within an otherwise benign system. This is a typical configuration where the traditional reliability index may provide misleading assurance of safety due to its insensitivity to tail behavior.

Problem Formulation

The structural model remains $g(R, S) = R - S$, but the load S is modeled as a two-component mixture to capture occasional extreme outcomes:

$$S \sim 0.999 \cdot \mathcal{N}(5, 2^2) + 0.001 \cdot \text{Pareto}(x_m = 10, \alpha = 1.5),$$

where the nominal component reflects the dominant, moderate loads, and the Pareto component introduces heavy-tailed outliers. The resistance is again normally distributed as $R \sim \mathcal{N}(20, 1.5^2)$.

This configuration creates a situation where the overall failure probability remains low, but when failure does occur, the resulting deficit is disproportionately large.

Results

Simulation yields:

Classical Reliability Index: $\beta = 3.3880$
 σ_g does not exist: so the E_f^* is undefined.
 Severity-Aware Index: Not computable (outside valid domain)

Interpretation

The classical index β indicates a highly reliable system with a failure probability of approximately 0.035%. However, this assessment is misleading, as evidenced by the extremely high value of E_f^* , which far exceeds the theoretical upper bound of ≈ 0.7979 that defines the interpretable domain of the Gaussian-based calibration function. Consequently, β_S is not defined for this case, which is defined as Extreme Severity (infinite variance).

This result is not an anomaly but a critical signal. The framework correctly identifies that failure events, though rare, possess a magnitude so large that they fall outside the conceptual reach of the standard Gaussian-benchmarked model. This property transforms β_S into a diagnostic tool: its incomputability functions as an alert for practitioners that a system may harbor catastrophic risks that evade detection by frequency-based metrics. Such a system demands further investigation and potentially more conservative design or alternative modeling.

4.4. Summary of Findings

The outcomes of the three numerical studies are compiled in [Table 2](#) for comparative analysis:

Table 2. *Summary of findings*

Example	System Description	Key Result	Interpretation
1. Consistency	Gaussian benchmark	$\beta_S \approx \beta$	Confirms alignment with classical reliability theory under ideal conditions.
2. Mild Failures	Frequent, low-severity events	$\beta_S > \beta$	Indicates favorable failure profile not penalized by the severity-aware metric.
3. Extreme Severity	Rare, catastrophic load events	β high, β_S undefined	Exposes hidden tail risk missed by traditional metrics; triggers diagnostic warning.

These findings emphasize that the β_S index is not merely a numerical extension but a conceptual enhancement of classical reliability theory. It retains consistency where appropriate, offers additional resolution in benign scenarios, and, most critically, detects latent high-risk phenomena that may otherwise remain concealed. The framework therefore provides engineers with a more nuanced and informative lens for structural safety assessment.

4.5. Case Study: Realistic Structural System with High but Quantifiable Severity

To further demonstrate the practical applicability of the proposed severity-aware framework, a case study involving a realistic structural member is examined. This example reflects an engineering design scenario where the system performs adequately under standard loading conditions, yet remains exposed to rare but severe live load events, which significantly elevate the consequences of failure.

4.5.1. Problem Formulation

The structural performance is described by the standard limit-state function

$$g(R, D, L) = R - (1.2D + 1.6L),$$

where R denotes the resistance, D the dead load, and L the live load. The random inputs are defined as follows:

Resistance R : Modeled by a Lognormal distribution with median 1520 and coefficient of variation 0.10, to capture the positive skew and non-negativity of material strength.

Dead Load D : Modeled as $D \sim \mathcal{N}(500, 50^2)$, representing a well-characterized permanent action.

Live Load L : Represented by a mixture of two Gumbel distributions:

$$L \sim \begin{cases} \text{Gumbel}(\mu = 150, \text{scale} = 30) & \text{with probability 0.9995,} \\ \text{Gumbel}(\mu = 500, \text{scale} = 30) & \text{with probability 0.0005.} \end{cases}$$

This formulation reflects typical usage scenarios dominated by moderate live loads, but occasionally perturbed by rare, high-intensity events, such as crowd surges, temporary overloads, or misestimation of service loads.

4.5.2. Simulation and Results

A Monte Carlo simulation with $N = 2,000,000$ samples was performed to estimate all reliability metrics. The key outcomes are summarized below:

- *Probability of Failure:* $p_f \approx 9.1 \times 10^{-5}$, corresponding to a classical reliability index of $\beta = -\Phi^{-1}(p_f) = 3.7442$.
- *Normalized Expected Failure Deficit:*

$$E_f^* = \frac{\mathbb{E}[-g(\mathbf{X}) \mid g(\mathbf{X}) < 0]}{\sigma_g} = 0.4741$$

This value is significantly elevated, reflecting severe failure consequences, but still lies within the admissible domain of the transformation function.

- *Severity-Aware Reliability Index:* Using the inverse mapping of

$$\frac{\varphi(b)}{\Phi(-b)} - b = E_f^*,$$

the corresponding severity-aware index is computed as $\beta_S = 1.2777$.

4.5.3. Interpretation and Implications

This case study reveals a risk scenario in which the classical index paints an overly optimistic picture. The high $\beta = 3.74$ reflects a rare probability of failure and would, in a conventional design context, imply excellent reliability. However, this conclusion is misleading, as it fails to account for the consequences of the rare failures.

The severity-aware index $\beta_S = 1.28$, derived from the normalized failure deficit, corrects this illusion by incorporating the magnitude of failure into the assessment. The sharp contrast between β and β_S demonstrates that even systems with rare failures may possess an unacceptable severity profile, thereby necessitating reevaluation.

This is not a case of extreme severity, where the deficit lies beyond the definable bounds of the framework. Instead, it is a case of high but quantifiable severity, where the framework not only flags the concern but also returns a meaningful index value. From an engineering standpoint, a value of $\beta_S = 1.28$ would be considered inadequate for critical structures, potentially prompting remedial actions such as structural reinforcement, design redundancy, or refined load control.

Thus, this example demonstrates that the value of β_S not merely as a quantitative reliability index, but as a diagnostic and interpretive tool for uncovering latent vulnerabilities obscured under classical formulations.

4.6. Visual Diagnostics of Failure Severity Across Risk Profiles

To complement the quantitative results presented earlier in Sec. 4, Fig. 6 provides a comparative visual analysis of three representative structural reliability scenarios. These were selected to span a broad spectrum of risk behavior, from classical Gaussian systems to ones with mild failure effects and finally to cases with extreme, hidden severity. Each row in Fig. 6 corresponds to one scenario: the left panels show the empirical distribution of the limit-state function g , while the right panels display the corresponding failure deficit distributions on a logarithmic scale.

Top Row (Fig. 6(1a,1b)): Classical Gaussian Case — $\beta \approx \beta_S \approx 3.50$, $E_f^ \approx 0.54$*

Fig. 6(1a,1b) illustrate the baseline Gaussian case. The limit-state distribution in Fig. 6(a) aligns nearly perfectly with the fitted Normal distribution, exhibiting symmetric tails and typical concentration near the mean. In Fig. 6(1b), the distribution of failure deficits (i.e., $-g$ for $g < 0$) confirms the absence of extreme severity. The deficit values cluster tightly, with a low mean of 0.54. This scenario demonstrates a situation where both failure frequency and failure magnitude are low and well-characterized, resulting in consistency between the classical reliability index β and the severity-aware index β_S .

Middle Row (Fig. 6(2a,2b)): Mild Failure Case — $\beta \approx 3.11$, $\beta_S \approx 3.84$, $E_f^ \approx 0.23$*

In this case, the system exhibits a higher failure probability, as seen in the denser left tail of Fig. 6(2a). Although the Normal approximation remains acceptable near the mean, deviations emerge near the threshold. Fig. 6(2b) reveals that these failures are consistently moderate: the deficit values remain bounded within a narrow range, with a mean of 0.93 and no significant outliers. This combination of higher frequency but relatively low consequence explains why $\beta_S > \beta$ here—the failures, while more likely, are less severe than a Gaussian failure assumption would suggest. The severity-aware framework interprets this correctly by assigning a higher index.

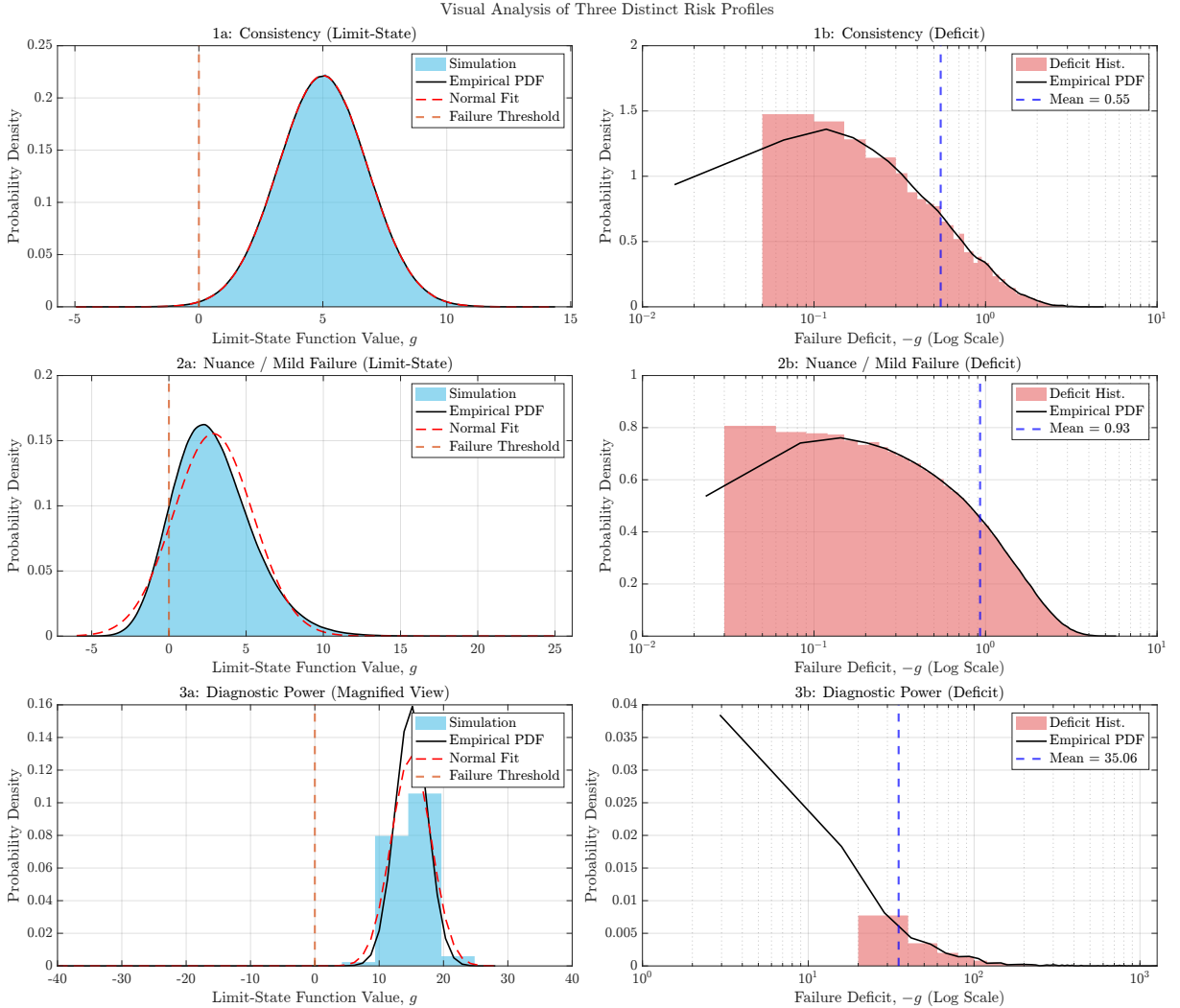


Figure 6. Visual comparison of three structural risk scenarios, using both limit-state function g distributions (left column) and corresponding failure deficit histograms for $g < 0$ (right column, log-scale). Top row (1a–1b): Gaussian benchmark case – $\beta \approx \beta_S \approx 3.50$, $E_f^* \approx 0.251$; symmetric tails and compact deficits yield consistent indices. Middle row (2a–2b): Mild failure case – $\beta \approx 3.11$, $\beta_S \approx 3.84$, $E_f^* \approx 0.235$; failure frequency increases, but severity remains bounded. Bottom row (3a–3b): Heavy-tailed case – $\beta \approx 3.14$, β_S undefined, $E_f^* = 1.67 > 0.7979$; catastrophic deficits cause diagnostic threshold violation. These visualizations illustrate the ability of the severity-aware framework to differentiate between benign and catastrophic failure behaviors, even when classical reliability metrics appear similar.

Bottom Row ([Fig. 6\(3a,3b\)](#)): Heavy-Tailed Case — $\beta \approx 3.14$, β_S undefined, $E_f^* = 1.67 > 0.7979$

This final case exposes the diagnostic strength of the severity-aware index. The main plot in [Fig. 6\(3a\)](#) gives the misleading impression of a symmetric and safe distribution. However, the inset reveals the hidden tail extending deeply into the negative domain, a heavy-tailed behavior not captured by the Gaussian fit. [Fig. 6\(3b\)](#) further demonstrates this: the deficit values span several orders of magnitude, with a mean of 42.16. The normalized deficit E_f^* exceeds the theoretical diagnostic limit of 0.7979, indicating that no equivalent Gaussian system could explain this severity level. The severity-aware index β_S is therefore undefined, not due to a computational failure, but as a deliberate signal that the system's risk lies outside the Gaussian paradigm. The classical β , while seemingly adequate, underestimates the catastrophic nature of possible outcomes.

5. A Severity Classification System for Risk-Informed Design

The previous sections have established that the Severity-Aware Reliability Index, β_S , supplements the classical reliability index β by introducing a measure that accounts for the depth or seriousness of failure consequences. Whereas β captures how frequently failure occurs, it cannot distinguish between a ductile, localized failure and a brittle, catastrophic one, even when both have equal probability. This section translates the abstract notion of normalized expected failure deficit, E_f^* , into a formal, interpretable severity classification system suitable for practical use in design and risk appraisal.

5.1. Derivation of Non-Arbitrary Severity Thresholds

A recurring criticism of novel metrics is the use of seemingly arbitrary thresholds for categorization. In this work, such arbitrariness is explicitly avoided by anchoring severity levels to reliability index values already familiar to practicing engineers. Instead of choosing cutoffs heuristically, thresholds are algorithmically derived by mapping classical reliability values to their corresponding failure deficit using the inverse transformation:

$$E_f^* = F(\beta_S) = \frac{\varphi(\beta_S)}{\Phi(-\beta_S)} - \beta_S,$$

This function is monotonic, invertible, and approaches a finite upper bound as $\beta_S \rightarrow 0$, with:

$$\lim_{\beta_S \rightarrow 0^+} E_f^* = \frac{2}{\sqrt{2\pi}} \approx 0.7979.$$

The thresholds for the classification levels are computed by evaluating E_f^* at reliability indices commonly used in practice (see [Fig. 7](#)):

$$\begin{aligned} \beta_S = 3.0 \quad (\text{standard target for high-reliability structures}) &\Rightarrow E_f^* \approx 0.283 \\ \beta_S = 2.0 \quad (\text{boundary for moderate-risk components}) &\Rightarrow E_f^* \approx 0.373 \\ \beta_S = 1.0 \quad (\text{rarely acceptable in structural design}) &\Rightarrow E_f^* \approx 0.525 \end{aligned}$$

This procedure guarantees that all category boundaries are reproducible, transparent, and theoretically sound.

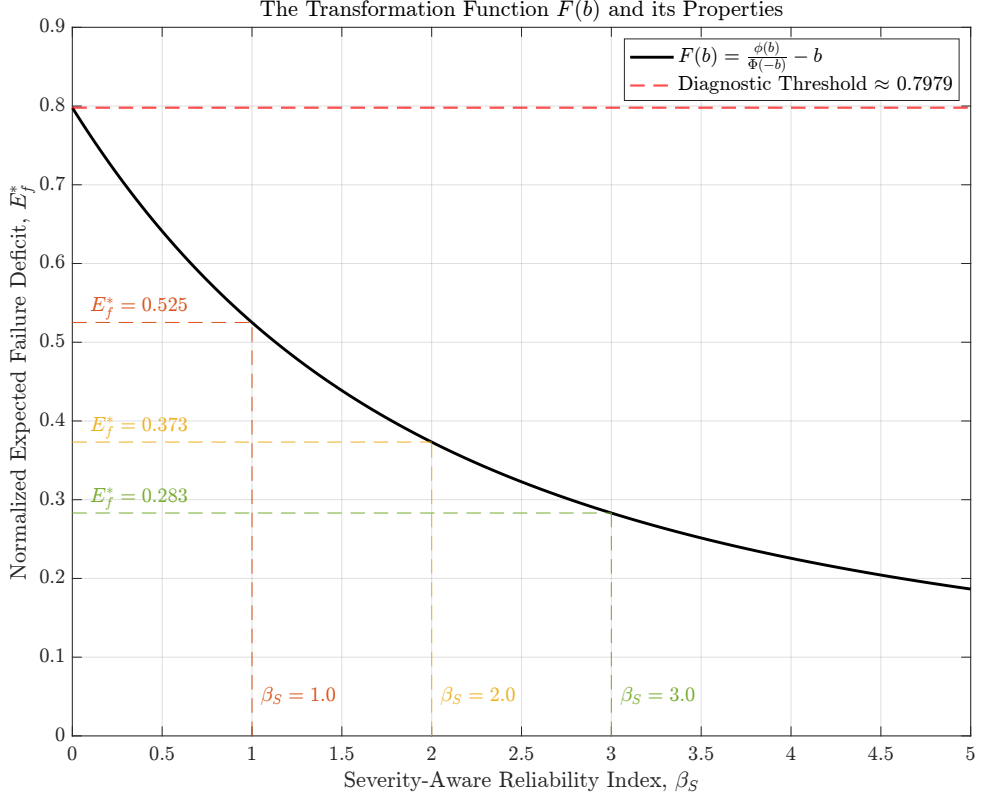


Figure 7. Severity thresholds and their corresponding expected failure deficits

5.2. Five-Level Severity Classification System

Based on the derived thresholds, we now propose a five-level severity scale (Table 3). The classification allows engineers to translate a single computed value of E_f^* into a qualitative risk interpretation, while preserving quantitative rigor.

The classification system can be applied across structural types and performance targets. Its interpretive power lies in exposing not only the frequency of failure, but also how physically damaging that failure is likely to be.

5.3. Relationship with Code-Based Risk Categorization

Current structural design codes, such as ASCE 7, already implement a risk-based framework by assigning structures to Risk Categories I through IV. These categories reflect the societal consequences of failure (e.g., a hospital vs. a warehouse), and influence the design via importance factors. These factors increase the applied loads and thereby elevate the required target reliability index β .

However, this system is qualitative and frequency-oriented. It ensures that failure becomes rarer, but not necessarily less damaging. Once failure occurs, ASCE 7 provides no means to assess whether the structural response is ductile and localized or brittle and widespread.

The severity classification system proposed in this study addresses this limitation directly. Rather than substituting existing design provisions, it offers a complementary diagnostic tool. Table 4 compares the two frameworks.

Table 3. *Proposed Severity Classification System*

Severity Level	β_S Range	E_f^* Range	Interpretation and Recommended Action
I: Mild	$\beta_S \geq 3.0$	$0 < E_f^* < 0.283$	Failure is gentle. Classical reliability index governs. No further mitigation required.
II: Moderate	$2.0 \leq \beta_S < 3.0$	$0.283 \leq E_f^* < 0.373$	Severity is perceptible. Enhanced quality assurance and optional monitoring may be prudent.
III: High	$1.0 \leq \beta_S < 2.0$	$0.373 \leq E_f^* < 0.525$	Severity is non-negligible. Consider design reinforcement or redundancy.
IV: Critical	$0 < \beta_S < 1.0$	$0.525 \leq E_f^* < 0.7979$	System approaches the risk boundary. Strengthening or redesign should be carried out.
V: Extreme	Incomputable	$E_f^* \geq 0.7979$	Catastrophic severity. Risk is beyond acceptable domain. Conceptual overhaul is necessary.

Table 4. *Comparison of Risk Categorization Approaches*

Feature	ASCE 7 Risk Categories	Severity-Based Classification (This Work)
Basis of Classification	Qualitative (use and occupancy)	Quantitative (failure deficit, E_f^*)
Targeted Property	Importance-driven reliability	Failure consequence depth
Mechanism	Indirect (load amplification)	Direct (severity evaluation)
Threshold Source	Prescriptive, code-defined	Computed from inverse Gaussian mapping
Tail Risk Visibility	Not visible	Explicitly detected when $E_f^* \geq 0.7979$

In practice, a two-step design workflow is recommended:

1. **Frequency Evaluation:** Use ASCE 7 (or relevant standard) to determine required β based on Risk Category. Ensure design meets this requirement.
2. **Severity Evaluation:** Compute E_f^* for the proposed design. Use [Table 3](#) to classify severity and determine if redesign or mitigation is warranted.

For non-critical structures, a severity classification of III or lower may be acceptable. For critical infrastructure, II or lower should be required. This dual assessment ensures that a design is not only reliable in the classical sense, but also resistant to high-consequence failures, therefore, satisfying both the frequency and the impact dimensions of structural risk.

5.4. A Practical Workflow for Integrated Frequency-Severity Assessment

To synthesize the severity classification framework with conventional design practices, this subsection presents a systematic workflow for severity-aware reliability assessment. The purpose is to guide engineers through a two-tiered validation process: first, a frequency-based verification aligned with existing code provisions; second, a severity-based diagnosis

enabled by the newly proposed metric E_f^* . The decision logic is summarized in the flowchart shown in Fig. 8.

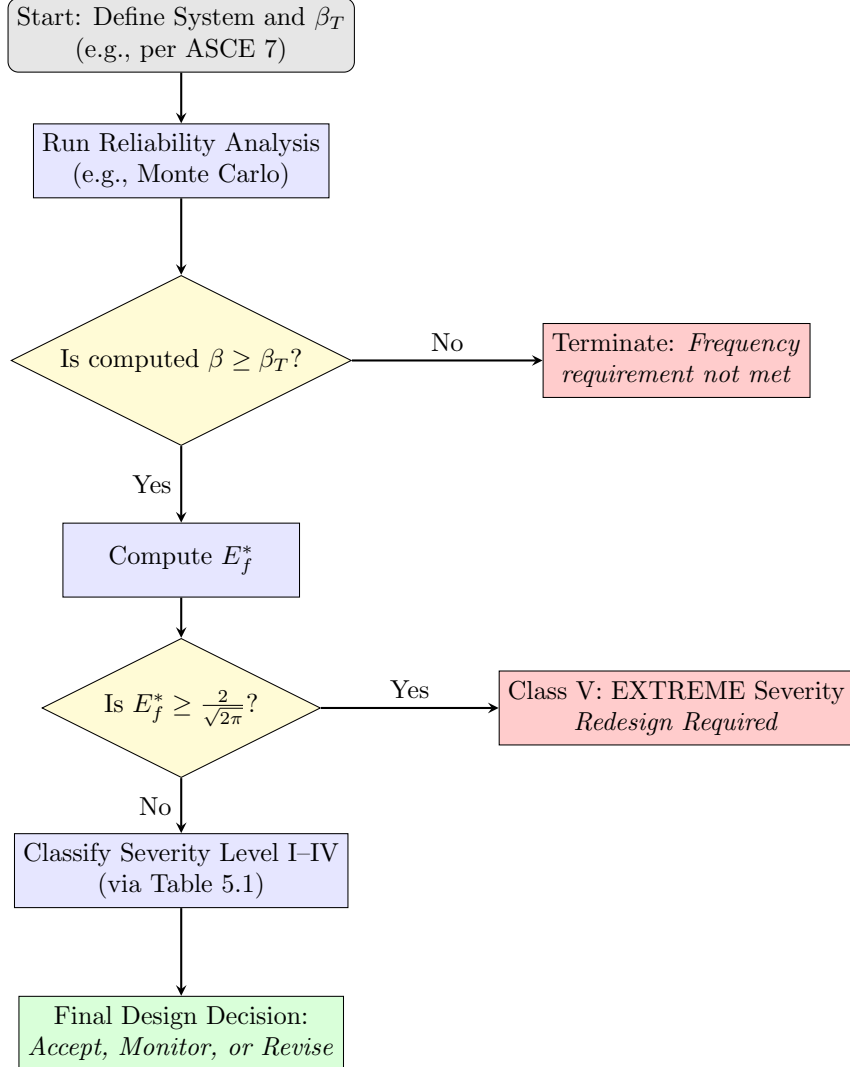


Figure 8. Workflow diagram for integrated reliability assessment combining traditional frequency metrics with severity-aware classification.

The workflow begins with the standard practice of establishing a target reliability index, β_T , according to code-based requirements (e.g., from ASCE 7 Risk Category assignments). Following this, a comprehensive reliability analysis is performed using appropriate probabilistic tools, such as Monte Carlo simulation.

The first validation checkpoint is a frequency check. Here, the computed classical reliability index, β , is compared against the prescribed target. If this requirement is not satisfied, the design is rejected, as it fails to meet the minimal frequency standard mandated by prevailing codes.

Only if the frequency condition is satisfied does the process advance to the severity check. At this stage, the normalized expected failure deficit, E_f^* , is calculated, capturing the depth of potential failure excursions. The pivotal diagnostic threshold then evaluates whether E_f^* exceeds the theoretical upper limit of the Gaussian-calibrated domain. If it does, the

design is classified as Level V: Extreme, indicating catastrophic, heavy-tailed risk that eludes detection by classical reliability indices. Such systems must be re-conceptualized or re-engineered entirely.

If the computed E_f^* lies below this critical bound, the severity level is then classified (Levels I-IV) using the ranges established in [Table 3](#). This step implicitly maps the value of E_f^* to the corresponding severity-aware reliability index, β_S . Finally, a holistic final design decision can be rendered based on both the successful frequency check and the now-quantified severity level. This may involve acceptance of the design, implementation of targeted monitoring strategies, or execution of further design refinements.

This structured process ensures that a design is not evaluated solely on the likelihood of failure but also on the magnitude of its consequences, hence delivering a more complete and risk-informed foundation for structural safety.

6. Discussion and Engineering Implications

This section provides an expanded interpretation of the new reliability index β_S , developed from the normalized Expected Failure Deficit E_f^* . We contrast its behavior with classical reliability metrics, emphasize its implications for engineering safety, and discuss the limitations and future prospects of this framework in practical risk assessment.

6.1. Comparison with Classical Reliability Index

Traditional structural reliability assessment relies on the probability of failure p_f , or the equivalent reliability index $\beta = -\Phi^{-1}(p_f)$, to quantify risk. These metrics capture how often a structure is expected to fail, assuming implicitly that all failures are of similar consequence. This modeling assumption simplifies calibration but disregards how severe a failure may be when it does occur.

The severity-aware index β_S , introduced in this study, addresses this shortcoming. It is constructed through the normalized conditional failure deficit:

$$E_f^* = \frac{\mathbb{E}[-g(\mathbf{X}) \mid g(\mathbf{X}) < 0]}{\sigma_g},$$

and defined implicitly by solving the transformation:

$$\frac{\varphi(\beta_S)}{\Phi(-\beta_S)} - \beta_S = E_f^*.$$

This formulation preserves interpretability under Gaussian conditions, where $\beta_S = \beta$, but detects deviations in tail behavior when failure severity is extreme. As demonstrated in [Sec. 4](#), systems with identical p_f but different deficit profiles yield markedly different β_S values. In the heavy-tailed case, we observed that although $\beta \approx 3.14$, the corresponding $E_f^* = 1.67$ exceeds the diagnostic threshold 0.7979, rendering β_S undefined. This contrast illustrates the inability of classical metrics to reflect rare but catastrophic scenarios.

The classical β gives a frequency-based impression of safety, but β_S complements it with a severity-adjusted perspective. Together, they form a richer picture of structural risk.

6.2. Practical Implications in Design and Decision-Making

The integration of failure severity via β_S has several practical implications:

Dual Risk Quantification: β_S enables simultaneous consideration of both failure probability and failure consequence, bridging a long-standing gap in reliability modeling. This is especially critical in safety-sensitive applications.

Early Warnings in Tail-Dominated Systems: Systems may appear safe under β , but an undefined or reduced β_S may signal dangerous tail behavior. This diagnostic capability serves as an early warning that traditional analyses might miss.

Rationalizing Redundancy and Design Margins: A structure with $\beta \geq 3$ but low or undefined β_S may warrant reconsideration. Engineers could use this signal to adjust safety factors or introduce mitigation strategies for extreme outcomes.

Reform of Design Standards: Risk-based codes that incorporate only p_f may be blind to rare, high-impact events. The proposed framework offers a feasible extension pathway by preserving compatibility with classical benchmarks.

Severity Classification: Sec. 5 proposed a severity classification system (Mild, Moderate, Severe, and Extreme) based on ranges of E_f^* . This classification offers a natural supplement to β_S and provides actionable insight: systems with Extreme severity ($E_f^* > 0.7979$) cannot be reliably characterized with Gaussian tools and may require fundamental design reevaluation.

6.3. On the Invertibility and Diagnostic Value of β_S

By construction, the transformation defining β_S is only invertible for

$$0 < E_f^* < \frac{2}{\sqrt{2\pi}} \approx 0.7979.$$

This bound is not a limitation but a feature: it identifies systems whose severity profiles cannot be matched by any Gaussian distribution. If a system yields $E_f^* > 0.7979$, the corresponding β_S becomes undefined, not due to computational failure, but because no equivalent Gaussian model can be constructed. Such cases require special scrutiny. The lack of a solution indicates a departure from conventional risk models. In such cases, engineers may consider adopting alternative characterizations such as:

- Truncated or heavy-tailed distributions.
- Nonparametric tail estimators.
- Conservative assignments (e.g., $\beta_S \rightarrow 0$) to reflect unquantifiable severity.

This diagnostic capacity distinguishes β_S from all classical indices.

6.4. Directions for Generalization

While β_S retains theoretical and practical consistency under Gaussian calibration, its application in broader contexts, such as skewed, heavy-tailed, or compound failure models, may require generalization. Future work may consider:

- Extending the transformation using alternative base distributions (e.g., Student-t, Laplace).

- Developing hybrid formulations that interpolate between Gaussian-based β_S and tail-aware surrogates.
- Exploring severity metrics based on tail-weighted moments or conditional risk integrals.

Such developments would widen the expressive range of the framework while preserving its diagnostic rigor.

6.5. Concluding Perspective

The severity-aware reliability index β_S offers a powerful yet interpretable generalization of classical reliability metrics. Its ability to remain consistent in the Gaussian regime and deviate meaningfully in non-Gaussian scenarios makes it particularly suitable for modern structural safety evaluations. When combined with the severity classification system proposed in Sec. 5 and supported by visual diagnostics (Sec. 4), it provides a comprehensive and actionable view of structural risk.

Importantly, the infeasibility of computing β_S for large E_f^* values is not a limitation; it is an indicator of profound risk mischaracterization under standard assumptions. This interpretive distinction equips engineers with a valuable signal that may otherwise go unnoticed in traditional assessments.

Through this diagnostic framing, β_S shifts the reliability paradigm from binary limit-state violation to a richer, consequence-informed view of safety, one that is more aligned with the actual stakes of structural performance.

7. Conclusions

This study introduced a new reliability index, β_S , designed to account not only for the probability of structural failure but also for the severity of such failure. Built upon the normalized Expected Failure Deficit E_f^* , the proposed measure provides a more informative representation of structural safety than the classical reliability index β , which captures frequency but ignores consequences.

It has been shown that β_S is consistent with the classical index in the Gaussian setting, where both measures coincide exactly, thus preserving theoretical compatibility under standard assumptions. However, in systems with skewed or heavy-tailed behavior, the new index exhibits sensitivity to high-consequence outliers that would remain hidden under conventional reliability models.

Our mathematical analysis established that β_S is well-defined for $E_f^* \in (0, 0.7979)$, a domain dictated by the invertibility of the defining transformation $F(b) = \frac{\varphi(b)}{\Phi(-b)} - b$. This upper bound is not an artifact but a diagnostic threshold: exceeding it implies that failure severity exceeds the descriptive capacity of Gaussian-based metrics. In such cases, the absence of a valid β_S solution reflects unquantifiable structural risk and signals that further modeling or re-design is warranted.

The numerical demonstrations emphasized that small failure probabilities can be misleading when associated with high conditional shortfalls. For instance, examples where $\beta \approx 3$ but β_S either dropped sharply or became undefined demonstrate a critical insight: the absence of frequent failure does not guarantee safety. The severity-aware index successfully identified these risks and offered early warnings that traditional methods could not provide.

To summarize the key contributions of this work:

- A new reliability index β_S incorporating both frequency and conditional failure severity, retaining theoretical consistency in Gaussian cases;
- A full analytical characterization of the transformation from E_f^* to β_S , including its invertibility limits and diagnostic behavior;
- Introduction of a severity classification system to support practical interpretation of E_f^* values, particularly in identifying systems operating in extreme regimes;
- Case studies demonstrating the divergence between β and β_S and revealing how the proposed metric exposes vulnerabilities obscured by conventional analysis.

Future research may aim to generalize the transformation framework to accommodate broader tail behaviors, enhance tail risk estimation, and examine how β_S may be embedded in reliability-informed design optimization, risk-based codes, or multi-hazard performance criteria.

Altogether, this work demonstrates that risk in structural systems is not merely a matter of how often failure occurs, but how severely. The index β_S provides engineers with a more sensitive and consequence-aware tool to identify, interpret, and mitigate structural vulnerabilities, especially in contexts where rare events may lead to disproportionate consequences.

Acknowledgments

This work was supported by the University of Sharjah, UAE. This support is highly appreciated by the authors.

Data Availability Statement

No external data was used in this research.

Competing Interests

The authors declare no competing financial interests or personal relationships that could have appeared to influence the work reported in this paper.

Author Contributions

Conceptualization: ML; Methodology: ML; Formal analysis and investigation: ML, SB, RA; Writing - original draft preparation: ML; Writing - review and editing: ML, SB, RA; Programming: ML.

References

- [1] T. V. Galambos. Load and resistance factor design (t.r. higgins award). *Engineering Journal*, 18(3):74–82, 1981.
- [2] Jochen Köhler, John D. Sørensen, and Bruce Ellingwood. Codes and standards for structural design - developments and future potential. *Structural Safety*, 113:102495, 2025. The Joint Committee of Structural Safety: past, present and a perspective on the future.

- [3] Andrzej S. Nowak. Calibration of lrfd bridge design code. Technical Report 368, Transportation Research Board, National Research Council, Washington, DC, 1999.
- [4] B. R. Ellingwood. Lrfd: implementing structural reliability in professional practice. *Engineering Structures*, 22(2):106–115, 2000.
- [5] Moussa Leblouba, S. Karzad, A. W. Tabsh, S. and S. Barakat. Plated versus corrugated web steel girders in shear: Behavior, parametric analysis, and reliability-based design optimization. *Buildings*, 12(12):2046, 2022.
- [6] Moussa Leblouba, Samer Barakat, Salah Altoubat, Mohamed Maalej, and Raghad Awad. Resistance factors for reliability based-design of fiber reinforced concrete suspended slabs in flexure. *Journal of Building Engineering*, 57:104911, 2022.
- [7] Moussa Leblouba and W. Tabsh, S. Reliability-based shear design of corrugated web steel beams for aisc 360 specification and csa-s16 standard. *Engineering Structures*, 215:110617, 2020.
- [8] Moussa Leblouba, W. Tabsh, S. and S. Barakat. Reliability-based design of corrugated web steel girders in shear as per aashto lrfd. *Journal of Constructional Steel Research*, 169:106013, 2020.
- [9] Raghad Awad, Samer Barakat, Moussa Leblouba, Salah Altoubat, and Mohamed Maalej. Reliability-based design of fiber reinforced concrete slabs-on-ground in flexure as per aci 360. *Structures*, 39:207–217, 2022.
- [10] Bruce Ellingwood, Marc Maes, F. Michael Bartlett, Andre T. Beck, Colin Caprani, Armen Der Kiureghian, Leonardo Dueñas-Osorio, Neryvaldo Galvão, Robert Gilbert, Jie Li, Jose Matos, Yasuhiro Mori, Iason Papaioannou, Roger Parades, Daniel Straub, and Bruno Sudret. Development of methods of structural reliability. *Structural Safety*, 113:102474, 2025. The Joint Committee of Structural Safety: past, present and a perspective on the future.
- [11] C. Allin Cornell. A probability-based structural code. *Journal Proceedings, American Concrete Institute*, 66(12):974–985, 1969.
- [12] Ove Dalager Ditlevsen and Henrik O. Madsen. *Structural Reliability Methods*. John Wiley & Sons Ltd, Chichester, UK, 1996.
- [13] Robert E. Melchers and André T. Beck. *Structural Reliability Analysis and Prediction*. John Wiley & Sons, 3rd edition, 2018.
- [14] Palle Thoft-Christensen and Michael J. Baker. *Structural Reliability Theory and Its Applications*. Springer-Verlag, Berlin and Heidelberg, 1982.
- [15] A. M. Hasofer and N. C. Lind. Exact and invariant second-moment code format. *Journal of the Engineering Mechanics Division*, 100(1):111–121, 1974.
- [16] Jianxu Su, Junping Zhang, Colin C. Caprani, and Junyong Zhou. A practical framework for determining target reliability indices for the assessment of existing structures based on risk-informed decision-making. *Structural Safety*, 114:102583, 2025.

- [17] Terje Aven. Risk analysis and management: Basic concepts and principles. *Reliability: Theory & Applications*, 4(1):57–73, 2009. Retrieved from https://www.gnedenko.net/Journal/2009/012009/RATA_1_2009-08.pdf.
- [18] William W. Lowrance. *Of Acceptable Risk: Science and the Determination of Safety*. William Kaufmann, Los Altos, CA, 1976.
- [19] M. H. Faber and M. G. Stewart. Risk assessment for civil engineering facilities: critical overview and discussion. *Reliability Engineering & System Safety*, 80(2):173–184, 2003.
- [20] Stanley Kaplan and Bruce J. Garrick. On the quantitative definition of risk. *Risk Analysis*, 1:11–27, 1981.
- [21] Dean H. Stamatidis. *Failure Mode and Effect Analysis: FMEA from Theory to Execution*. Quality Press, 2003.
- [22] Darrell Duffie and Jun Pan. An overview of value at risk. *Journal of Derivatives*, 4(3):7–49, 1997.
- [23] R. Tyrrell Rockafellar and Stanislav Uryasev. Optimization of conditional value-at-risk. *Journal of Risk*, 2:21–42, 2000.
- [24] A. Chaudhuri, M. Norton, and B. Kramer. Risk-based design optimization via probability of failure, conditional value-at-risk, and buffered probability of failure. In *AIAA SciTech 2020 Forum*, page 2130, 2020.
- [25] Y. Xu and P. Wang. Cvar formulation of reliability-based design problems considering the risk of extreme failure events. In *2021 Annual Reliability and Maintainability Symposium (RAMS)*, pages 1–5, 2021.
- [26] C. Filippi, G. Guastaroba, and M. G. Speranza. Conditional value-at-risk beyond finance: a survey. *International Transactions in Operational Research*, 27:1277–1319, 2020.
- [27] Armengol Gasull and Frederic Utzet. Approximating mills ratio. *Journal of Mathematical Analysis and Applications*, 420(2):1832–1853, 2014.